Glacial Iron Sources Stimulate the Southern Ocean Carbon Cycle

C. Laufkötter[1,2,3] (ID), Alon A. Stern[1] (ID), Jasmin G. John[4] (ID), Charles A. Stock[4] (ID), and John P. Dunne[4] (ID)

[1]Program in Atmospheric and Oceanic Sciences, Princeton University, Princeton, NJ, USA, [2]Climate and Environmental Physics, Physics Institute, University of Bern, Bern, Switzerland, [3]Oeschger Centre for Climate Change Research, University of Bern, Bern, Switzerland, [4]National Oceanic and Atmospheric Administration/Geophysical Fluid Dynamics Laboratory, Princeton, NJ, USA

Abstract Icebergs and glacial meltwater have been observed to significantly affect chlorophyll concentrations, primary production, and particle export locally, yet the quantitative influence of glacial iron on the carbon cycle of the Southern Ocean remains unknown. We analyze the impact of icebergs and glacial meltwater on the Southern Ocean carbon cycle in a global Earth System Model. We consider several simulations spanning low and high bounds of current estimates of glacial iron concentration. We find that a high glacial iron input produces the best agreement with observed iron and chlorophyll distributions. These high glacial iron input results indicate that about 30% of the Southern Ocean particle export production, that is, the flux of particulate organic matter through the 100 m depth level, is driven by glacial iron sources. This export production is associated with an uptake of 0.14 Pg carbon per year, which reduces carbon outgassing in the Southern Ocean by 30%.

Plain Language Summary Icebergs and glacial meltwater from Antarctica contain significant amounts of iron, which is important for phytoplankton growth and marine production in the iron-limited Southern Ocean. Since phytoplankton growth is connected to the carbon cycle, glacial iron sources are assumed to influence the Southern Ocean carbon cycle. However, this influence has not been quantified yet. We use a global Earth System Model to analyze the impacts of icebergs and glacial meltwater on the Southern Ocean carbon cycle. We calculate several simulations using low and high bounds of current estimates of glacial iron concentration. In our model, a high glacial iron input produces the best agreement with observed iron and chlorophyll distributions. These high glacial iron input results indicate that about 30% of the carbon export to depth is driven by glacial iron sources in the Southern Ocean, associated with a 30% reduction in carbon outgassing. Our results indicate that glacial iron plays a significant role in Southern Ocean carbon cycling and oceanic carbon uptake.

1. Introduction

The Southern Ocean is an important player in the global carbon cycle because of its unique physical and biogeochemical properties. In particular, a disproportionally large amount of anthropogenic carbon is taken up south of 35°S (Frölicher et al., 2015; Sabine et al., 2004). The majority of the Southern Ocean is limited by the micronutrient iron during the growth season (Moore et al., 2013). Adding dissolved iron to the Southern Ocean stimulates large phytoplankton blooms (e.g., Boyd & Trull, 2007) that may lead to substantial export events (Smetacek et al., 2012). Icebergs and glacial meltwater contain significant amounts of bioavailable iron (Death et al., 2014; Raiswell, 2011; Raiswell et al., 2008, 2016), with the overall estimated iron input from glacial sources and dust being of similar scale—albeit with large uncertainties regarding the amount, solubility, and bioavailability (Boyd et al., 2012). Field studies and satellite observations show that icebergs are associated with higher chlorophyll concentrations (Duprat et al., 2016), phytoplankton biomass (Schwarz & Schodlok, 2009), primary production (Wu & Hou, 2017), and krill and seabirds (Smith & Yamanaka, 2007). Moreover, an increased flux of particulate organic matter has been observed in Lagrangian sediment traps beneath a large tabular icebergs (Smith et al., 2011).

First attempts to model the biogeochemical impact of icebergs and glacial meltwater on the Southern Ocean have focused on their influence on chlorophyll and primary production. Results from Lancelot et al. (2009)

Table 1

Global and Southern Ocean Annual dFe Flux for All Iron Sources Used in the Experiments and for Comparison the Range of Global dFe Fluxes Commonly Used in Biogeochemistry Models (From Tagliabue et al., 2016, Representing Values From 13 Different Marine Biogeochemistry Models)

Iron source	Global dFe flux [Gmol Fe/year]	global dFe flux used in different models [Gmol Fe/year]	Southern Ocean (< 50° S) [Gmol Fe/year]
Dust deposition	13.8	1.4–32.7	0.28
Sediments	250–256	0.6–194	3.8–5.2
Iceberg meltwater	–	–	0.05–0.5
Iceberg-hosted sediments	–	–	1.94
Glacial Meltwater	–	–	0.06–0.6

Note. For the glacial sources, upper and lower bounds of the tested values are given. We did not change the parameterization of the sediment source, however the sediment iron flux depends on the carbon flux at the sea-floor, which increases with higher glacial iron inputs. We therefore also give the upper and lower bounds for the sediment flux. All iron sources enter the ocean at the surface except for the sediment flux, which enters the ocean at the sea-floor.

suggest that icebergs cause up to 25% of chlorophyll in areas influenced by icebergs. Simulations by Death et al. (2014) suggest that icebergs and glacial meltwater increase Southern Ocean primary production by up to 40%. Wadley et al. (2014) estimate that icebergs drive between 6% and 10% of Southern Ocean primary production, using an eddy-resolving ocean model that parameterizes iron inputs from dust, sediments, icebergs, and sea ice. The potential impact of glacial iron sources on export production and oceanic carbon uptake has not yet been quantified.

In this study we use a global coupled carbon-climate Earth System Model to simulate the Southern Ocean carbon cycle under different assumptions for the iron concentration in icebergs and glacial meltwater. We perform a thorough model evaluation using recently available iron and chlorophyll measurements and we analyze how glacial iron sources influence the biological productivity, carbon export, and oceanic carbon uptake.

2. Methods

To estimate the impact of glacial iron sources on the carbon cycle, we force the global coupled climate-carbon Earth System Model ESM2M (Dunne et al., 2012, 2013) with estimates for the iron flux from icebergs and glacial meltwater. The modeled spatial resolution is 1°, with slightly higher resolution at the Equator. ESM2M is coupled to the ecosystem model COBALT (Stock et al., 2014) to simulate the marine iron cycling and the impacts on primary and export production. A detailed model description can be found in Stock et al. (2014), we restrict ourselves here to the components most relevant for iron cycling. COBALT computes the free Fe concentration that can be scavenged based on Parekh et al. (2004). A linear scavenging rate and a single ligand model is used, with a reduced stability of Fe-ligand complexes under light. Biological iron uptake is proportional to the growth rate of an organism and ambient iron concentrations, allowing for varying Fe/C ratios. One particulate Fe pool is implemented and the remineralization efficiency is reduced relative to organic material resulting in a remineralization depth-scale beyond that for sinking organic material.

Originally, ESM2M-COBALT considers two sources of iron: atmospheric dust deposition and sedimental iron inputs. The atmospheric dust deposition is represented using a dust climatology based on Fan et al. (2006) and Moxim et al. (2011). The sedimental iron source depends on sedimentary carbon oxidation rates and bottom water oxygen concentrations, following Dale et al. (2015). An overview on the magnitude of the iron sources is shown in Table 1, and the geographical pattern of the iron sources is shown in Figure 1.

We have extended the original COBALT iron forcing to include iron from icebergs and glacial meltwater. To this end, we use GFDL's ESM2G (Dunne et al., 2012, 2013) to calculate a preindustrial climatology of the frozen precipitation over the Antarctic continent, which is then instantaneously routed to the coast along hydraulic potential pathways. We divide this frozen flux into an iceberg flux and a meltwater flux, following the ratio suggested in Rignot et al. (2013). The meltwater is released immediately into the ocean around Antarctica's coast. The iceberg flux is divided into multiple icebergs, represented as Lagrangian particles (Martin & Adcroft,
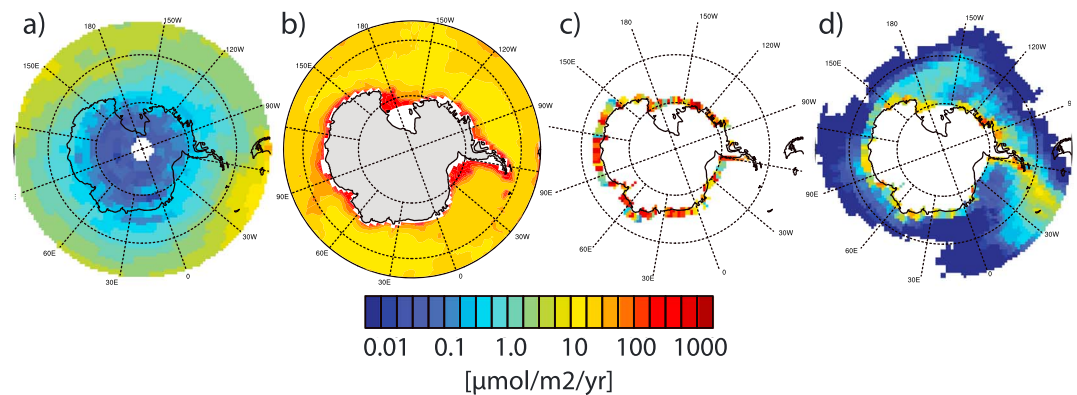
Figure 1. Annual mean iron forcing from (a) dust, (b) sediments, (c) glacial meltwater, and (d) icebergs south of 50°S.

2010; Stern et al., 2016). The icebergs then drift into the ocean where they gradually melt and release freshwater. The modeled iceberg distribution has similar orders of magnitude and a similar spatial structure compared to observational estimates (Tournadre et al., 2016), a thorough discussion can be found in Martin and Adcroft (2010) and Stern et al. (2016). COBALT currently does not parameterize iron from sea ice.

Current observations of the iron concentration in iceberg and glacial meltwater span orders of magnitude. We therefore run simulations using the upper and lower end of reported values. For the iron concentration in glacial meltwater, we use values from Death et al. (2014), who compare previously reported meltwater iron concentrations and use values between 3 and 30 µmol Fe per liter. For the iron concentration in icebergs, we use values between 5 and 50 nmol Fe per liter based on Raiswell et al. (2008). In addition to the iron contained in the meltwater, icebergs contain layers of sediment which have very high iron concentrations: up to 0.076 wt.% of the iceberg-hosted sediment might be bioavailable iron (Raiswell et al., 2016). However, the few available observations indicate that the sediment content of icebergs varies strongly (Hopwood et al., 2017; Raiswell et al., 2016). In addition, it is not well understood what fraction of the iron in the iceberg sediments is soluble and bioavailable (Boyd et al., 2012). We therefore consider an additional scenario in which we assume a small fraction of the icebergs (0.01%) consists of sediments, which have an 0.01% soluble iron content. These percentages represent the lower end of recent observations (Raiswell et al., 2016) and therefore constitute a rather conservative estimate. We have also tested higher percentages, however in our model this results in unrealistically high iron concentrations in the Southern Ocean and the simulations have therefore been discarded. We acknowledge that there might be substantial variability in iceberg-hosted sediments which we cannot reproduce.

2.1. Experiments

We present four model experiments which vary in the amount of iron contained in icebergs and glacial meltwater. Experiment "No Ice" serves as a control run in which no iron inputs from glacial iron sources are considered. Experiment "Ice Low" contains low iron concentrations in icebergs (5 µmol/m^3) and in glacial meltwater (3 mmol/m^3). Ice Medium contains high iron concentrations in icebergs and glacial meltwater (50 µmol/m^3 and 30 mmol/m^3, respectively). For the Ice High simulations, we additionally assume that 0.01% of the iceberg contains sediments. We spun up the model in preindustrial control mode (i.e., fixed 1850 forcing) for 1000 years using the Ice Low forcing until the model is in equilibrium and drift in the air-sea CO$_2$ flux and carbon export is negligible. We use the preindustrial scenario to avoid mixing the response to changes in iceberg-iron forcing with the response to changing atmospheric CO$_2$ concentrations. We then run an additional 100 model years for each of the experiments considered. The first 70 years of the extended experiments are considered spin-up and we analyze the last 30 years of simulation.

3. Model Evaluation

To evaluate the model, we compare the simulated fields of dissolved iron (dFe) and chlorophyll with dFe measurements and satellite-based chlorophyll estimates. Model studies indicate no significant changes in chlorophyll, NPP, and export production in the past 50 years in the Southern Ocean (Laufkötter et al., 2013). In addition, comparisons of preindustrial and historical COBALT simulations also show only small differences in Southern Ocean dFe, chlorophyll, and export production (not shown). We therefore feel that validating the
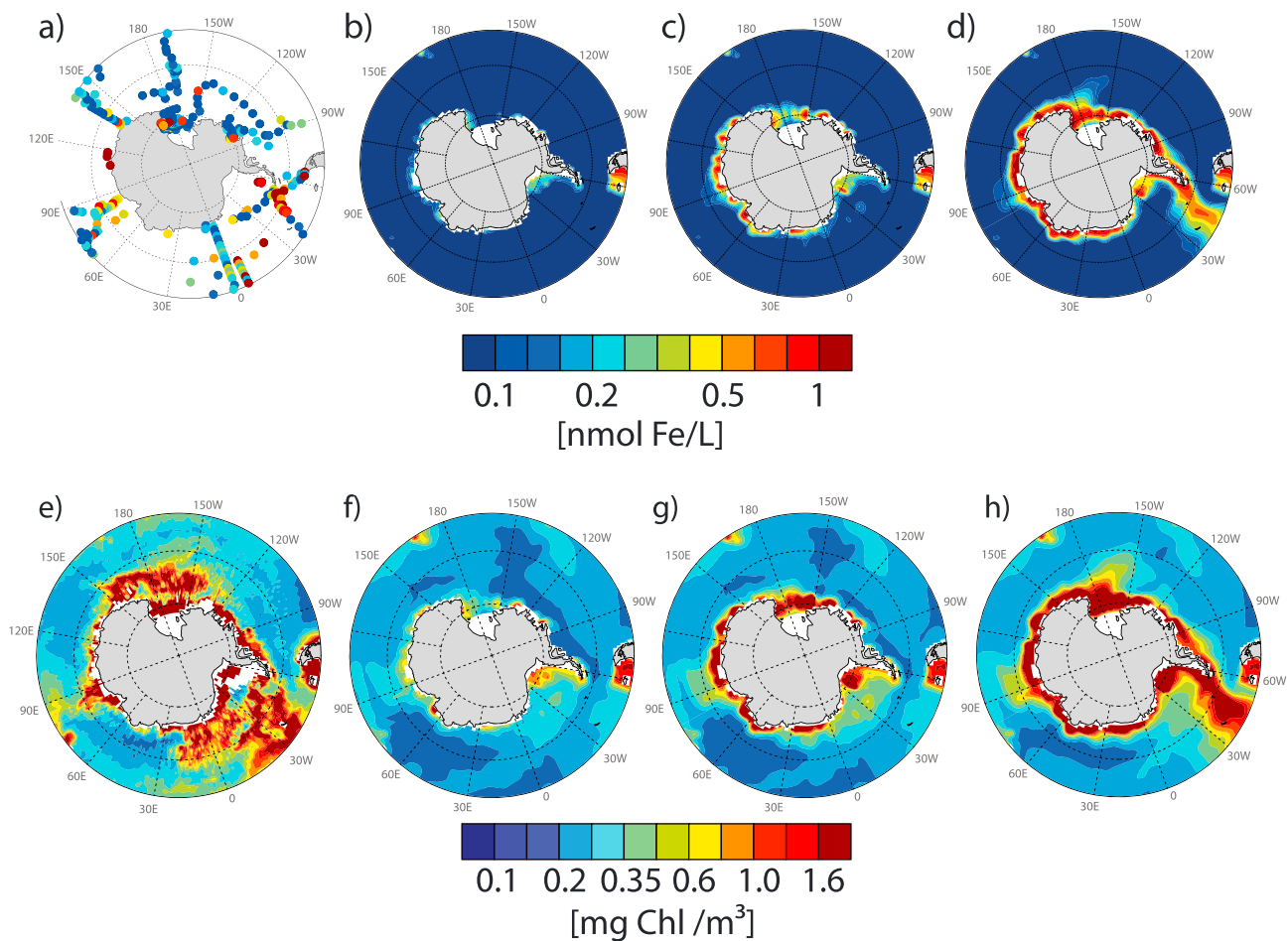
Figure 2. (a) Observed dissolved iron concentrations (top 50 m, south of 50°S) from the GEOTRACES intermediate data product (Schlitzer et al., 2018; Tagliabue et al., 2012) combined. (b)–(d) Spring-autumn mean surface dissolved iron concentration in the Ice Low, Ice Medium, and Ice High scenarios, respectively. (e) Satellite-based estimates of annual mean surface chlorophyll concentration south of 50°S from Johnson et al. (2013). (f)–(h) Spring-autumn mean surface chlorophyll concentration in the ice low, medium, and high scenarios, respectively. We do not show the No Ice experiment as it is visually almost identical to the Low Ice experiment. We have removed the winter months from the model output to account for the summer bias in the observations (see main text). Note the logarithmic scale.

model against the first-order large-scale present-day characteristics of the Southern Ocean is reasonable. For dFe, we use observations from the GEOTRACES intermediate data product (Schlitzer et al., 2018) combined with the dFe database published in Tagliabue et al. (2012). Surface maps of observed and modeled dFe are shown in Figures 2a–2d. Due to harsh environmental conditions, the observations are biased toward summer, we therefore removed the winter months from the model output and compare the observations against the modeled spring-summer-autumn mean. We concentrate on the upper 50 m as this is where the glacial iron sources mostly affect production. The observed dFe concentration between 50 and 1,000 m depth ranges between 0.1 and 0.25 nmol Fe per liter, which is captured in all experiments.

The observations indicate very low dFe concentrations (less than 0.2 nmol Fe per liter) in most parts of the open Southern Ocean which is captured in all three model experiments, although all experiments slightly underestimate the surface iron concentration. Close to the Antarctic coast and outward of the Antarctic Peninsula, the observations indicate high iron concentrations (1 nmol Fe per liter and higher). This pattern is best captured in the Ice High scenario. The Ice Medium and Ice Low scenario miss the high iron values outward of the Antarctic Peninsula, the Ice Low scenario also miss the higher iron values close to the Antarctic coast. The observed standard deviation (calculated in log space and then converted back) is 2.6 nmol Fe per liter, which is captured in the Ice High scenario (2.7 nmol Fe per liter), while it is considerably lower in the Ice Medium and Ice Low scenario (2.1 and 1.7 nmol Fe per liter, respectively). All simulations have a negative bias compared to the observations, but the bias is substantially reduced in Ice High (−0.04, −0.05, and −0.07 nmol Fe per liter

for Ice High, Medium, and Low, respectively, the observed mean is 0.37 nmol Fe per liter). According to these metrics, the Ice High scenario matches the observations best.

Figures 2e–2h compare annual mean modeled surface chlorophyll concentrations with satellite-based estimates. Due to cloud coverage and the sun angle, which in winter prevents satellite measurements of water leaving irradiance in the Southern Ocean, the satellite-based estimates are biased toward summer. We therefore again removed the winter months from the model output and compare the observations against the modeled spring-summer-autumn mean. The satellite estimate (Johnson et al., 2013) suggests high chlorophyll values (>1.5 mg Chl per cubic meter) in the vicinity of the Antarctic coast and also in the Weddell Sea and the Ross Sea (>1.0 mg Chl per cubic meter), extending northward up to 60°S at the Ross Sea and up to 50°S at the Wedell Sea. Apart from these areas, chlorophyll levels are generally low with values between 0.1 and 0.3 mg Chl per cubic meter.

The Ice Low simulation generally underestimates chlorophyll levels in all regions. The Ice Medium simulation shows notably higher chlorophyll concentrations around Antarctica with values of up to 1.0 mg Chl per cubic meter, but the values are still lower than suggested by the satellite data, additionally the simulation does not capture the high chlorophyll regions in the Weddell and Ross Sea. The Ice High simulation is the best match to the satellite estimate, showing a plume of high chlorophyll concentration in the areas that have high iceberg concentrations, that is, extending outward from the Antarctic Peninsula and also into the northern part of the Ross Sea. The Spearman rank correlation between simulated and satellite-based chlorophyll is 0.53, 0.59, and 0.67 for Ice Low, Ice Medium, and Ice High simulations, respectively. The model generally underestimates chlorophyll, but the bias is significantly smaller in simulations with high iceberg-iron inputs: The average observed chlorophyll concentration in areas receiving iron flux from icebergs is 1.05 mg Chl per cubic meter, the bias in the Ice Low, Medium, and High simulations is −0.68, −0.49, and −0.17 mg Chl per cubic meter, respectively (again calculated in log space and then transformed back).

4. Export Production and Carbon Uptake Driven by Glacial Iron Sources

Figures 3a–3d show the flux of particulate organic carbon through the 100 m depth level (export production) in the four model experiments. The increasing levels of surface iron availability in the four experiments are clearly reflected by increasing levels of export production. In the No Ice and Ice Low runs, the distribution and total amount of export production is almost indistinguishable and mostly low (values below 1.8 mol·m^{-2}·year^{-1}) except for the water above the Patagonian shelf where iron concentrations are high (>3 mol·m^{-2}·year^{-1}) due to sedimentary iron inputs. The overall annual export production in the No Ice and Ice Low experiments is 0.55 and 0.56 PgC per year, respectively, for the area south of 50°S. In the Ice Medium experiment, the iron inputs from glacial iron sources leave a clear imprint in the vicinity of the Antarctic coast with particle flux locally exceeding 3 mol·m^{-2}·year^{-1}. Particle export is also slightly higher in the open ocean. The overall export production south of 50°S increases to 0.65 PgC per year. In the Ice High experiment, the high export flux around the Antarctic continent is even more pronounced. Additionally, open ocean values are significantly higher, particularly in regions where a large number of icebergs pass through (outward of the Antarctic Peninsula). The overall export production south of 50°S in the Ice High experiment is 0.81 PgC per year. Compared to 0.55 PgC per year in the No Ice experiment, the amount of export production driven by glacial iron sources in Ice High is 0.26 PgC per year or about 30% of the total particle export production.

The pattern of particulate organic carbon flux through the 1,000 m depth level (not shown) mostly reflects the carbon flux at 100 m depth, with carbon flux at 1,000 m depth in the Ice High run being about 30% higher compared to the No Ice simulation. This suggests that a significant fraction of the particle export production driven by glacial iron sources reaches the deep ocean, potentially removing carbon from the atmosphere for centuries.

Figures 3e–3h show the air-sea CO_2 flux in the four model experiments. The Southern Ocean is mostly outgassing in these preindustrial simulations, except for the water close to the Antarctic coast where a small net uptake of CO_2 occurs. When switching on the iron from glacial sources, this area around Antarctica gradually takes up more carbon, reducing the outgassing by roughly 30% from 0.4 PgC per year in the No Ice simulation to 0.26 PgC per year in the Ice High simulation.
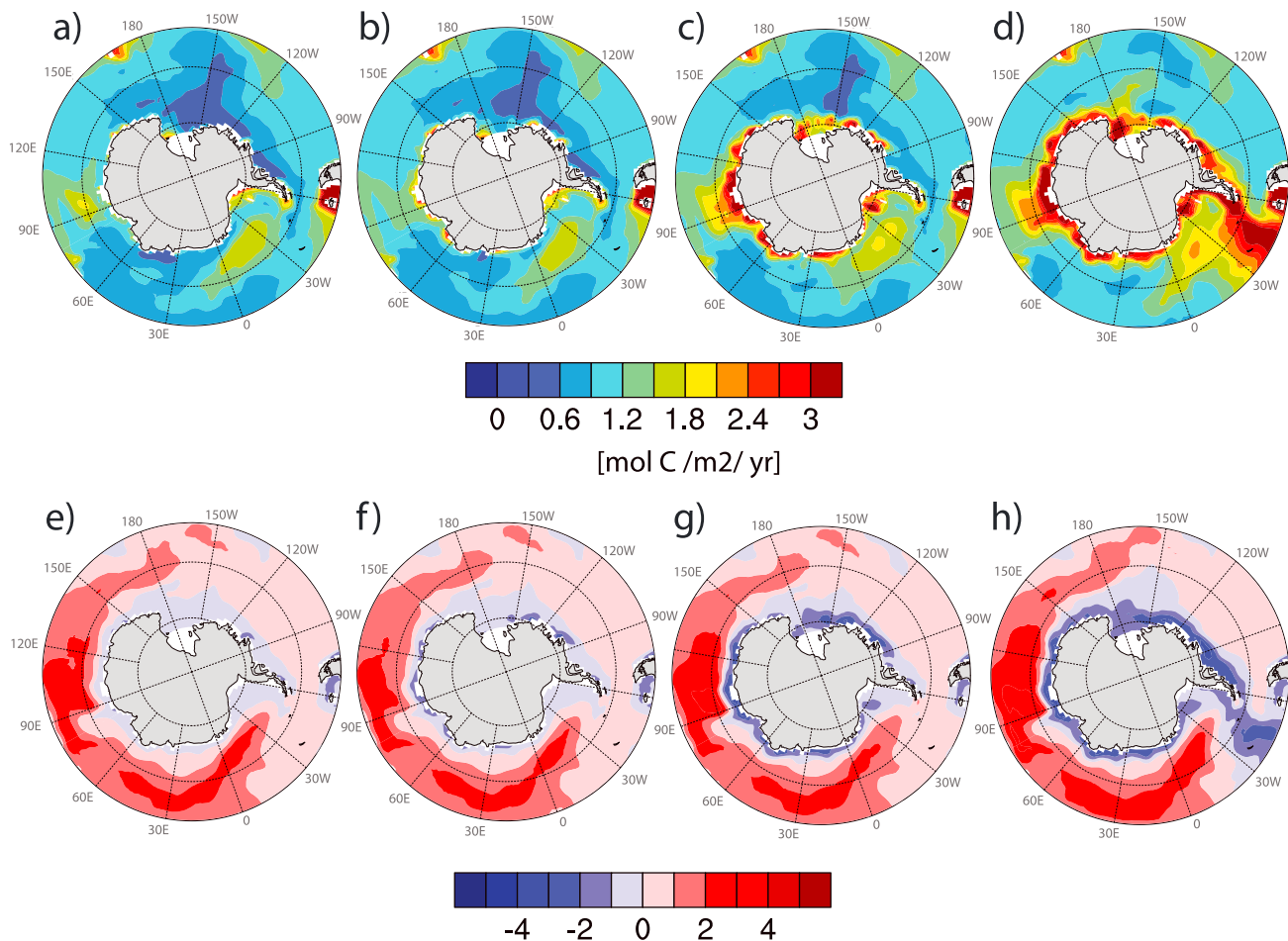
Figure 3. Modeled annual mean particle export through 100 m depth for (a) a scenario with no glacial iron input, (b)–(d) the ice low, medium, and high scenarios, respectively. Air-sea CO₂ flux south of 50°S in (e) a model simulation without glacial iron sources and (f)–(g) the ice low, medium, and high experiments, respectively. Red colors indicate flux out of the ocean, blue colors indicate flux into the ocean.

5. Discussion and Conclusion

Our model suggests a significant contribution of glacial iron sources to the Southern Ocean carbon cycle—in the scenario most consistent with observations, about 30% of the export production is driven by glacial iron sources, associated with a 30% decrease in carbon outgassing. The only observational estimate for carbon export driven by glacial iron sources comes from Duprat et al. (2016), who use satellite observations to show that chlorophyll levels are significantly enhanced in the wake of giant icebergs. Assuming an increase in carbon export by a factor of 5–10, they estimate that about 20% of export production in the Southern Ocean might be due to giant iceberg fertilization. This value is similar in magnitude, albeit somewhat lower than the 30% our model predicts. Duprat et al. (2016) do not include the effects of glacial meltwater in their estimate, which might be the reason for our higher estimate.

However, there are severe uncertainties in the parameterization of all aspects of the iron cycling, including the magnitude and variability of iron inputs from dust, sediments, and glacial iron sources, the solubility and bioavailability of the iron, the role of sea ice, the iron chemistry in the ocean including iron scavenging and ligand binding, biological iron cycling, iron remineralization, and interaction with particles (Boyd et al., 2012; Hopwood et al., 2017; Lannuzel et al., 2016; Raiswell et al., 2016; Tagliabue et al., 2016). Furthermore, models are struggling to correctly represent Southern Ocean circulation which has implications for the amount of upwelled iron and also for the light availability for phytoplankton via stratification which in turn affects iron uptake. Tagliabue et al. (2016) demonstrated that global biogeochemical models can have the same Fe cycle features with very different values of sources and residence times. Consequently, previous model studies analyzing the importance of glacial iron sources for biological production (Death et al., 2014; Lancelot et al.,

2009; Wadley et al., 2014) reached differing conclusions regarding the importance of icebergs and glacial meltwater. While Lancelot et al. (2009) and Death et al. (2014) report potentially strong contributions of icebergs to biological production (10–50% and 40%, respectively), Wadley et al. (2014) find only a contribution of 6–10%. These stark differences are caused by different parameterizations of the iron cycling, including the magnitude and pattern of iceberg and sedimental iron input, parameterizations of iron chemistry, biological uptake, and particle dynamics. Furthermore, limited available observations only weakly constrained model evaluation.

Due to the new GEOTRACES data and improved satellite chlorophyll estimates we are able to show that model skill in simulating both surface iron and chlorophyll concentrations significantly improve when including iron sources from icebergs and glacial meltwater. This step, which could not be carried out in previously published analyses, builds confidence in our estimate of the magnitude of carbon flux associated with glacial iron. However, we cannot rule out that the improved model skill could also be achieved by a combination of other factors, such as higher sediment inputs, improved representation of Southern Ocean circulation, slower scavenging, or the representation of sea ice.

The large observed variability especially in iron from iceberg-hosted sediments is likely to lead to a small-scale spatial variability in export production that our model is not able to reproduce. In addition, very little is known about the time scales of release of the basal sediments, which might be lost quickly in the vicinity of the ice shelf. Specific observations are needed to better constrain this important flux. In this study we choose comparatively low values for the averaged amount of sediments in icebergs, thus we hope to obtain a conservative estimate for the regional response in export production.

We use a comparatively high sediment iron source (see Table 1), therefore we assume that we rather overestimate than underestimate the sedimental iron input. Despite this high sediment source we do not find elevated iron and chlorophyll levels above the Antarctic shelf in the No Ice and Low Ice scenario, suggesting that most of the sedimental iron input does not directly impact the surface ocean. Our results are in line with a recent study from Graham et al. (2015), who showed that satellite-derived surface chlorophyll is neither enhanced above upwelling at fronts nor above areas of shallow bathymetry (<1,000 m) in the Southern Ocean, concluding that iron from deep sources is unlikely to directly enter the surface ocean. However, we acknowledge that circulation models struggle to correctly represent Southern Ocean water masses and their exchange via upwelling, mixing, and entrainment (Heuzé et al., 2013; Sallée et al., 2013), which could strongly influence the amount of dissolved iron that is upwelled.

COBALT has a rapid iron scavenging compared to other models, reflecting the relatively high iron inputs from sediments and dust. The resulting fast iron removal from the surface ocean might favor surface iron sources such as dust and glacial sources over deep sea entrainment. On the other hand, we would generally expect high dust and sediment inputs to reduce the relative importance of icebergs, yet our results suggested the importance of icebergs despite high iron inputs. The magnitude of iron scavenging and its potential variability is arguably the least constrained component of the iron cycling (Tagliabue et al., 2016) and constitutes a major uncertainty in current model studies of glacial iron sources.

A further limitation of our study is the missing representation of iron from sea ice, which is an important iron buffering mechanism in a previous model study (Wang et al., 2014). While sea ice is estimated to be a smaller iron source than icebergs (Wang et al., 2014) and has been shown to be a minor contributor to iron sources on the West-Antarctic Peninsula shelf (Annett et al., 2017), it might still play an important role in other regions of the Southern Ocean and it is possible that a part of the iron that we allocate to icebergs and glacial meltwater comes from melting sea ice.

Finally, parameterizations of carbon export in the Southern Ocean are based on very few measurements. While our model suggests a strong reaction of biological production and carbon export to higher iron inputs, observations suggest a complex set of responses of the plankton community and the subsequent carbon export to iron fertilization (Martin et al., 2013; Pollard et al., 2009; Shaw et al., 2011; Smetacek et al., 2012; Smith et al., 2011) and current ecosystem models vary strongly in their parameterization of carbon fluxes (Laufkötter et al., 2015, 2016). An improved understanding of Southern Ocean ecosystems might reveal more complex relationships between iron inputs and carbon cycling than currently simulated. Furthermore, as our model simulations exclusively differ in the amount of glacial iron input, the differences in oceanic CO_2 uptake between the simulations is directly due to the biological response to iron fertilization. The simulated pattern

of air-sea CO_2 flux shows a strong CO_2 uptake signal in iceberg-affected regions. Estimates of preindustrial CO_2 uptake are not detailed enough to judge whether this pattern in the CO_2 uptake distribution is realistic. Even present-day air-sea CO_2 flux observations are sparse in the Southern Ocean and the flux estimates vary wildly (Gray et al., 2018).

A definitive answer to the relative importance of the different iron sources is beyond the scope of a single model study. Our contribution is to show that including iron from icebergs can significantly improve model-data fit of surface iron and chlorophyll and that the biological response to iron fertilization from icebergs can possibly have a significant impact on the Southern Ocean carbon cycle.

References

Annett, A. L., Fitzsimmons, J. N., Séguret, M. J., Lagerström, M., Meredith, M. P., Schofield, O., & Sherrell, R. M. (2017). Controls on dissolved and particulate iron distributions in surface waters of the Western Antarctic Peninsula shelf. *Marine Chemistry*, *196*, 81–97. https://doi.org/10.1016/j.marchem.2017.06.004

Boyd, P. W., Arrigo, K. R., Strzepek, R., & Van Dijken, G. L. (2012). Mapping phytoplankton iron utilization: Insights into Southern Ocean supply mechanisms. *Journal of Geophysical Research*, *117*, 1–18. https://doi.org/10.1029/2011JC007726

Boyd, P., & Trull, T. (2007). Understanding the export of biogenic particles in oceanic waters: Is there consensus? *Progress In Oceanography*, *72*(4), 276–312. https://doi.org/10.1016/j.pocean.2006.10.007

Dale, A., Nickelsen, L., Scholz, F., Hensen, C., Oschlies, A., & Wallmann, K. (2015). A revised global estimate of dissolved iron fluxes. *Global Biogeochemical Cycles*, *29*, 691–707. https://doi.org/10.1002/2014GB005017

Death, R., Wadham, J. L., Monteiro, F., Le Brocq, A. M., Tranter, M., Ridgwell, A., et al. (2014). Antarctic ice sheet fertilises the Southern Ocean. *Biogeosciences*, *11*(10), 2635–2643. https://doi.org/10.5194/bg-11-2635-2014

Dunne, J. P., Hales, B., & Toggweiler, J. R. (2012). Global calcite cycling constrained by sediment preservation controls. *Global Biogeochemical Cycles*, *26*, GB3023. https://doi.org/10.1029/2010GB003935

Dunne, J. P., John, J. G., Shevliakova, E., Stouffer, R. J., Krasting, J. P., Malyshev, S. L., et al. (2013). GFDL's ESM2 global coupled climate—Carbon earth system models. Part II: Carbon system formulation and baseline simulation characteristics*. *Journal of Climate*, *26*(7), 2247–2267. https://doi.org/10.1175/JCLI-D-12-00150.1

Duprat, L. P. A. M., Bigg, G. R., & Wilton, D. J. (2016). Enhanced Southern Ocean marine productivity due to fertilization by giant icebergs. *Nature Geoscience*, *9*, 219–221. https://doi.org/10.1038/ngeo2633

Fan, S. M., Moxim, W. J., & Levy, H. (2006). Aeolian input of bioavailable iron to the ocean. *Geophysical Research Letters*, *33*, L07602. https://doi.org/10.1029/2005GL024852

Frölicher, T. L., Sarmiento, J. L., Paynter, D. J., Dunne, J. P., Krasting, J. P., & Winton, M. (2015). Dominance of the Southern Ocean in anthropogenic carbon and heat uptake in CMIP5 models. *Journal of Climate*, *28*(2), 862–886. https://doi.org/10.1175/JCLI-D-14-00117.1

Graham, R. M., De Boer, A. M., van Sebille, E., Kohfeld, K. E., & Schlosser, C. (2015). Inferring source regions and supply mechanisms of iron in the Southern Ocean from satellite chlorophyll data. *Deep-Sea Research Part I: Oceanographic Research Papers*, *104*, 9–25. https://doi.org/10.1016/j.dsr.2015.05.007

Gray, A. R., Johnson, K. S., Bushinsky, S. M., Riser, S. C., Russell, J. L., Talley, L. D., et al. (2018). Autonomous biogeochemical floats detect significant carbon dioxide outgassing in the high-latitude Southern Ocean. *Geophysical Research Letters*, *45*, 9049–9057. https://doi.org/10.1029/2018GL078013

Heuzé, C., Heywood, K. J., Stevens, D. P., & Ridley, J. K. (2013). *Southern Ocean bottom water characteristics in CMIP5 models*, *40*, 1409–1414. https://doi.org/10.1002/grl.50287

Hopwood, M., Cantoni, C., Clarke, J., Cozzi, S., & Achterberg, E. (2017). The heterogeneous nature of Fe delivery from melting icebergs. *Geochemical Perspectives Letters*, *3*, 200–209. https://doi.org/10.7185/geochemlet.1723

Johnson, R., Strutton, P. G., Wright, S. W., McMinn, A., & Meiners, K. M. (2013). Three improved satellite chlorophyll algorithms for the Southern Ocean. *Journal of Geophysical Research: Oceans*, *118*, 3694–3703. https://doi.org/10.1002/jgrc.20270

Lancelot, C., de Montety, A., Goosse, H., Becquevort, S., Schoemann, V., Pasquer, B., & Vancoppenolle, M. (2009). Spatial distribution of the iron supply to phytoplankton in the Southern Ocean: A model study. *Biogeosciences*, *6*(3), 4919–4962. https://doi.org/10.5194/bgd-6-4919-2009

Lannuzel, D., Vancoppenolle, M., van der Merwe, P., de Jong, J., Meiners, K., Grotti, M., et al. (2016). Iron in sea ice: Review and new insights. *Elementa: Science of the Anthropocene*, *4*, 000130. https://doi.org/10.12952/journal.elementa.000130

Laufkötter, C., Vogt, M., & Gruber, N. (2013). Long-term trends in ocean plankton production and particle export between 1960–2006. *Biogeosciences*, *10*(11), 7373–7393. https://doi.org/10.5194/bg-10-7373-2013

Laufkötter, C., Vogt, M., Gruber, N., Aita-Noguchi, M., Aumont, O., Bopp, L., et al. (2015). Drivers and uncertainties of future global marine primary production in marine ecosystem models. *Biogeosciences*, *12*(4), 3731–3824. https://doi.org/10.5194/bgd-12-3731-2015

Laufkötter, C., Vogt, M., Gruber, N., Bopp, L., Dunne, J., Hauck, J., et al. (2016). Projected decreases in future marine export production: The role of the carbon flux through the upper ocean ecosystem. *Biogeosciences*, *13*(4), 4023–4047. https://doi.org/doi:10.5194/bgd-12-3731-2015

Martin, T., & Adcroft, A. (2010). Parameterizing the fresh-water flux from land ice to ocean with interactive icebergs in a coupled climate model. *Ocean Modelling*, *34*(3-4), 111–124. https://doi.org/10.1016/j.ocemod.2010.05.001

Martin, P., van der Loeff, M. R., Cassar, N., Vandromme, P., D'Ovidio, F., Stemmann, L., et al. (2013). Iron fertilization enhanced net community production but not downward particle flux during the Southern Ocean iron fertilization experiment LOHAFEX. *Global Biogeochemical Cycles*, *27*, 1–11. https://doi.org/10.1002/gbc.20077

Moore, C. M., Mills, M. M., Arrigo, K. R., Berman-Frank, I., Bopp, L., Boyd, P. W., et al. (2013). Processes and patterns of oceanic nutrient limitation. *Nature Geoscience*, *6*(9), 701–710. https://doi.org/10.1038/ngeo1765

Moxim, W. J., Fan, S. M., & Levy, H. (2011). The meteorological nature of variable soluble iron transport and deposition within the North Atlantic Ocean basin. *Journal of Geophysical Research*, *116*, 1–26. https://doi.org/10.1029/2010JD014709

Parekh, P., Follows, M. J., & Boyle, E. (2004). Modeling the global ocean iron cycle. *Global Biogeochemical Cycles*, *18*, GB1002. https://doi.org/10.1029/2003GB002061

Pollard, R. T., Salter, I., Sanders, R. J., Lucas, M. I., Moore, C. M., Mills, R. A., et al. (2009). Southern Ocean deep-water carbon export enhanced by natural iron fertilization. *Nature*, *457*(7229), 577–80. https://doi.org/10.1038/nature07716

Raiswell, R. (2011). Iceberg-hosted nanoparticulate Fe in the Southern Ocean: Mineralogy, origin, dissolution kinetics and source of bioavailable Fe. *Deep-Sea Research Part II: Topical Studies in Oceanography*, *58*(11–12), 1364–1375. https://doi.org/10.1016/j.dsr2.2010.11.011

Raiswell, R., Benning, L. G., Davidson, L., & Tranter, M. (2008). Nanoparticulate bioavailable iron minerals in icebergs and glaciers. *Mineralogical Magazine*, *72*(1), 345–348. https://doi.org/10.1180/minmag.2008.072.1.345

Raiswell, R., Hawkings, J. R., Benning, L. G., Baker, A. R., Death, R., Albani, S., et al. (2016). Potentially bioavailable iron delivery by iceberg-hosted sediments and atmospheric dust to the polar oceans. *Biogeosciences*, *13*, 3887–3900. https://doi.org/10.5194/bg-2016-20

Rignot, E., Jacobs, S., Mouginot, J., & Scheuchl, B. (2013). Ice shelf melting around Antarctica. *Science*, *1*(June), 1–15. https://doi.org/10.1126/science.1235798

Sabine, C. L., Feely, R. A., Gruber, N., Key, R. M., Lee, K., Bullister, J. L., et al. (2004). The oceanic sink for anthropogenic CO2. *Science*, *305*(5682), 367–71. https://doi.org/10.1126/science.1097403

Sallée, J., Shuckburgh, E., Bruneau, N., Meijers, A. J. S., Bracegirdle, T. J., Wang, Z., & Roy, T. (2013). Assessment of Southern Ocean water mass circulation and characteristics in CMIP5 models: Historical bias and forcing response. *Journal of Geophysical Research: Oceans*, *118*, 1830–1844. https://doi.org/10.1002/jgrc.20135

Schlitzer, R., Anderson, R. F., Dodas, E. M., Lohan, M., Geibert, W., Tagliabue, A., et al. (2018). The GEOTRACES intermediate data product 2017. *Chemical Geology*, *493*, 210–223. https://doi.org/10.1016/j.chemgeo.2018.05.040

Schwarz, J. N., & Schodlok, M. P. (2009). Impact of drifting icebergs on surface phytoplankton biomass in the Southern Ocean: Ocean colour remote sensing and in situ iceberg tracking. *Deep-Sea Research Part I: Oceanographic Research Papers*, *56*(10), 1727–1741. https://doi.org/10.1016/j.dsr.2009.05.003

Shaw, T. J., Smith, K. L., Hexel, C. R., Dudgeon, R., Sherman, A. D., Vernet, M., & Kaufmann, R. S. (2011). 234Th-based carbon export around free-drifting icebergs in the Southern Ocean. *Deep-Sea Research Part II: Topical Studies in Oceanography*, *58*(11-12), 1384–1391. https://doi.org/10.1016/j.dsr2.2010.11.019

Smetacek, V., Klaas, C., Strass, V. H., Assmy, P., Montresor, M., Cisewski, B., et al. (2012). Deep carbon export from a Southern Ocean iron-fertilized diatom bloom. *Nature*, *487*(7407), 313–319. https://doi.org/10.1038/nature11229

Smith, K. L., Sherman, A. D., Shaw, T. J., Murray, A. E., Vernet, M., & Cefarelli, A. O. (2011). Carbon export associated with free-drifting icebergs in the Southern Ocean. *Deep-Sea Research Part II: Topical Studies in Oceanography*, *58*(11-12), 1485–1496. https://doi.org/10.1016/j.dsr2.2010.11.027

Smith, S. L., & Yamanaka, Y. (2007). Optimization-based model of multinutrient uptake kinetics. *Limnology and Oceanography*, *52*(4), 1545–1558. https://doi.org/10.4319/lo.2007.52.4.1545

Stern, A. A., Adcroft, A., & Sergienko, O. (2016). The effects of Antarctic iceberg calving-size distribution in a global climate model. *Journal of Geophysical Research: Oceans*, *121*, 5773–5788. https://doi.org/10.1002/2016JC011835.Received

Stock, C. a., Dunne, J. P., & John, J. G. (2014). Global-scale carbon and energy flows through the marine planktonic food web: An analysis with a coupled physical—biological model. *Progress in Oceanography*, *120*, 1–28. https://doi.org/10.1016/j.pocean.2013.07.001

Tagliabue, A., Aumont, O., DeAth, R., Dunne, J. P., Dutkiewicz, S., Galbraith, E., et al. (2016). How well do global ocean biogeochemistry models simulate dissolved iron distributions? *Global Biogeochemical Cycles*, *30*, 149–174. https://doi.org/10.1002/2015GB005289

Tagliabue, A., Mtshali, T., Aumont, O., Bowie, A. R., Klunder, M. B., Roychoudhury, A. N., & Swart, S. (2012). A global compilation of dissolved iron measurements: Focus on distributions and processes in the Southern Ocean. *Biogeosciences*, *9*(6), 2333–2349. https://doi.org/10.5194/bg-9-2333-2012

Tournadre, J., Bouhier, N., Girard-Ardhuin, F., & Rémy, F. (2016). Antarctic iceberg distributions 1992–2014. *Journal of Geophysical Research: Oceans*, *121*, 327–349. https://doi.org/10.1002/2015JC011070.Received

Wadley, M. R., Jickells, T. D., & Heywood, K. J. (2014). The role of iron sources and transport for Southern Ocean productivity. *Deep-Sea Research Part I: Oceanographic Research Papers*, *87*, 82–94. https://doi.org/10.1016/j.dsr.2014.02.003

Wang, S., Bailey, D., Lindsay, K., Moore, J. K., & Holland, M. (2014). Impact of sea ice on the marine iron cycle and phytoplankton productivity. *Biogeosciences*, *11*(17), 4713–4731. https://doi.org/10.5194/bg-11-4713-2014

Wu, S. Y., & Hou, S. (2017). Impact of icebergs on net primary productivity in the Southern Ocean. *Cryosphere*, *11*(2), 707–722. https://doi.org/10.5194/tc-11-707-2017